YU ISSN 0015—3206
FZKAAA 22 (1) 153 (1990)

MULTIGAMMA-RAY CALIBRATION STANDARDS

RICHARD A. MEYER*

Division of Nuclear Physics, U. S. Department of Energy, Washington, D. C. 20585, USA

and

Nuclear Chemistry Division, Lawrence Livermore National Laboratory, Livermore, California 94550, USA

Received 29 September 1989

UDC 539.166

Original scientific paper

We have calibrated a self-consistent set of multigamma-ray standards using the automated multi-spectrometer γ-ray counting facility at LLNL's Nuclear Chemistry Division. Pure sources of long-lived activity were produced by mass separation and/or chemical purification. The sources were counted individually and in combination on several different calibrated spectrometer systems. These systems utilize various detectors ranging from small (X-ray) detectors to large volume high-purity Ge detectors. This has allowed the use of the most ideal individual detector-efficiency characteristics for the determination of the relative γ-ray intensities. Precise energy measurements, reported earlier$^{1)}$, have been performed by an independent method. Both the energy and γ-ray-emission probabilities we determine compare well with independently established values such as the recent ICRM intercomparison of ^{152}Eu. We discuss our investigations aimed at resolving the shape of the efficiency response function up to 10 MeV for large volume Ge (Li) and high-purity Ge detectors. Recent results on the γ-ray-emission probabilities per decay for ^{149}Gd and ^{168}Tm multigamma-ray sources are discussed. For ^{168}Tm, we deduce a 0.01% β^- branch to the 87.73-keV level in ^{168}Yb rather than the previous value which was a factor of 200 greater. In addition, we describe current cooperative efforts aimed at establishing a consistent set of data for short-lived fission products. Included are recent measurements on the bromine fission products with γ-rays up to 7 MeV.

---

* Permanent address: ER-23 GTN, Division of High Energy and Nuclear Physics, U. S. Department of Energy, Washington, D. C. 20585.

1. Introduction

The ideal calibration source for a γ-ray spectrometer is a single, long-lived radioactive nuclide possessing a large number of equally intense γ-rays at evenly-spaced energy intervals. Such a source enables repeated energy and efficiency calibration mesaurements to bc made on automated multispectrometer analytical systems. In research, the geometry of the source with respect to the detector and attenuating materials can vary widely within a single experiment, necessitating several separate calibration measurements. Although no ideal calibration source has been found, several long-lived radioactive isotopes have proven useful compromises. In an effort to develop a self-consistent set of multigamma-ray calibration sources we have made measurements of precise γ-ray energy and emission probability values, and have characterized the efficiency of Ge (Li) and high-purity Ge detectors up to 10 MeV. Our initial results have appeared in unpublished tables2) and preliminary reports1,3,4). Our values are in good agreement with those of other investigators5–7). Here we review the procedures we have used to determine these values and give our present values. In addition, we cite some recent measurements of shorter-lived activities present in fission products which emit high-energy γ-rays.

It is important to note that the γ-ray-emission probabilities we present in this report are the result of measurement of each source on several different spectrometers with different efficiency characteristics. In addition, intersource calibration was performed. Sources of established multigamma-ray standards such as ^{152}Eu also were counted simultaneously with, for example, ^{168}Tm. In this way any local variation in the detector efficiency or counting conditions could be checked.

2. Spectroscopy techniques

Most sources used in the measurements were both chemically purified and mass separated. For some nuclides, such as ^{152}Eu, sources were prepared by two cycles of chemical purification followed by mass separation. Spectral data were accumulated with several spectrometer systems employing a variety of detectors and standard pulse-processing electronic components. The spectra analyses were performed using the code GAMANAL by Gunnink and coworkers8–10). This code divides spectrum analysis into two parts: first, the reduction of the spectral features into understandable entities such as peak energies and areas, and secondly, the quantitative interpretation of these items as disintegration rates or atoms of specific nuclides at a specified time.

If one were to consider a hypothetical detector system exhibiting no instrumental noise or dispersion, all of the full-energy pulses corresponding to a given γ-ray would appear in one channel rather than as a broadened distribution. The background just before the γ-ray peak consits of degraded full-energy events resulting from such effects as »trapping« in the detector and low angle scattering by the source or materials surrounding it. These background events continue right up to the full-energy peak, with the result being a discontinuity or step in the level of the background. Any processes that disperse the original narrow γ-ray peak width will also smooth the background discontinuity. In GAMANAL, a procedure which closely represents the detector process initially establishes a background including step functions with the discontinuities occurring at the peak positions and with step heights proportioned according to the approximate peak heights. The background is subsequently smoothed with two or three cycles of linear smoothing.

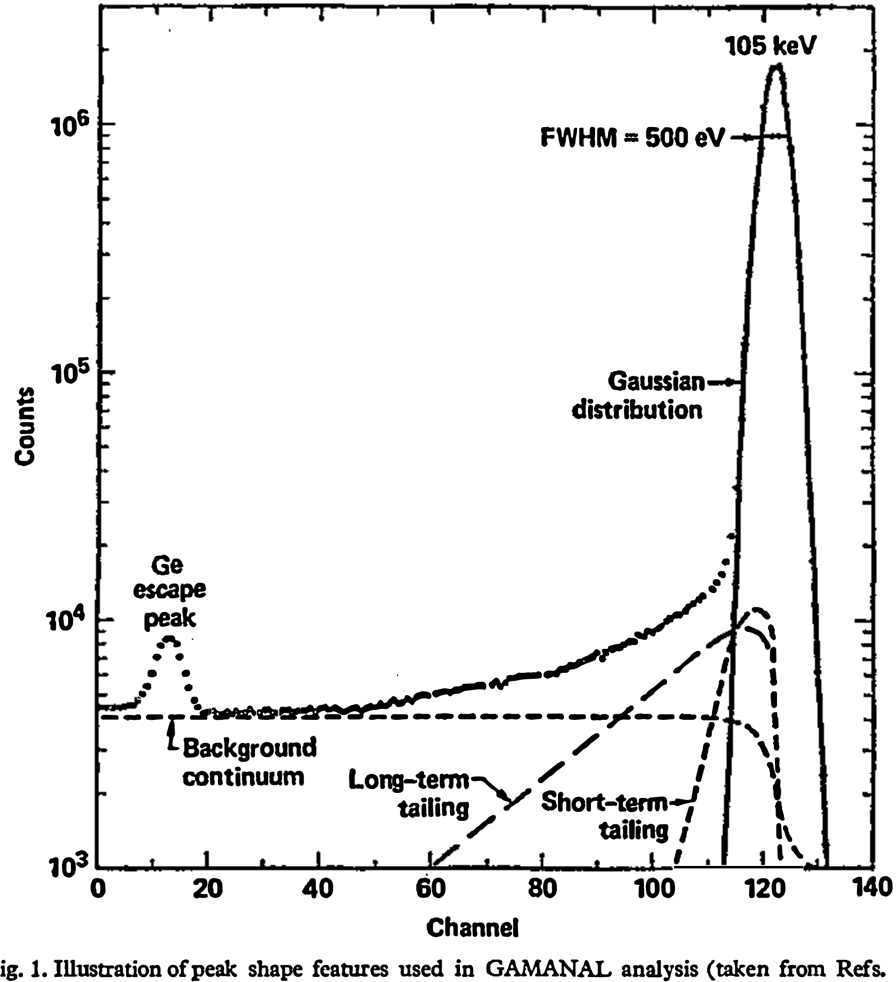

Fig. 1. Illustration of peak shape features used in GAMANAL analysis (taken from Refs. 8, 9 and 11).

There are at least three distinct components in the observed shape of a γ-ray peak. These are illustrated in Fig. 1. Additional structure may result from improper usage or alignment of the electronic components of the system. The major portion of the peak can be described by a Gaussian function. However, accurate data analysis requires that the »short-term« tailing, in particular, not be ignored. The »long-term« tailing may be important in the analysis of some complex multiplets. Otherwise, it can frequently be treated as part of the background as is done in GAMANAL. Gunnink has developed an algorithm which adequately fits the observed peak shapes. Techniques have been devised[11] whereby all of the peak shape parameters can be fixed from fitting two widely separated peaks in a spectrum.

The simultaneous fitting of several peaks in a multiplet is generally accomplished by some iterative method. For example, GAMANAL linearizes the fit equations by using a Taylor's expansion about the trial solution and then uses a Newton-Raphson or Gauss iterative technique. Very complicated γ-ray multiplets can be unfolded using this approach[11].

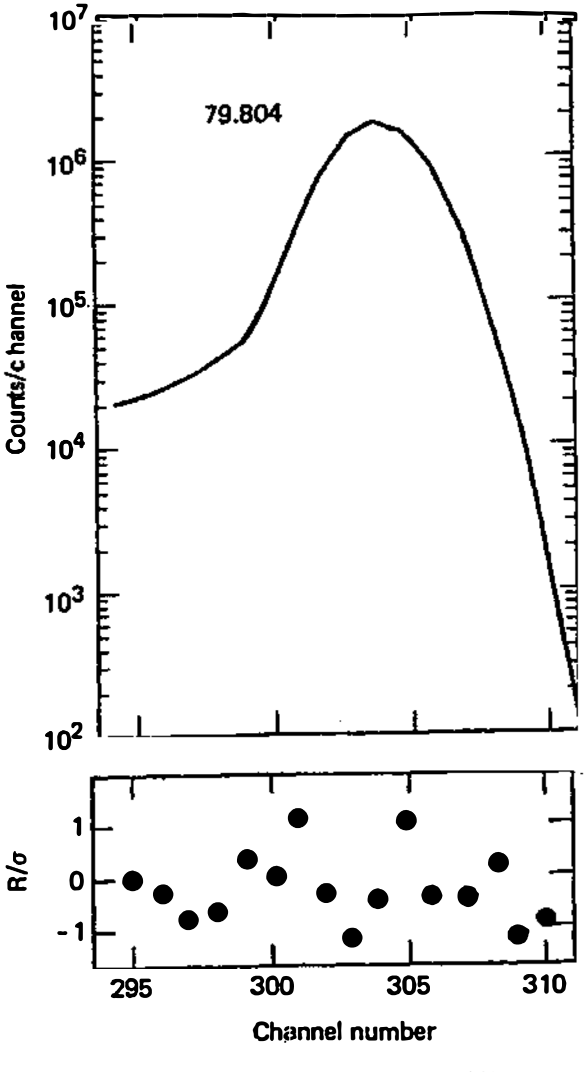

Fig. 2. GAMANAL peak shape fit to 79.804-keV photopeak of ^{168}Tm (showing excess of 10^6 counts in peak channel).

An example of the spectral analysis can come from our recent investigation of 93-day ^{168}Tm. In Figs. 2 and 3 we show the GAMANAL fit to the intense 79- and 184-keV γ-ray peaks. These figures illustrate one other feature of the LLNL automated systems. When a channel location exceeds one million events, the channel overflow is registered in the control computer and identified with the particular spectrum. These channels are later corrected when the spectra are analyzed on larger computers thereby extending the statistics by which an individual peak can be measured. Figures 4 and 5 illustrate the sensitivity with which doublet peaks can be resolved. In all the measurements presented here, the photopeak shape parameters were fit individually to each spectrum.

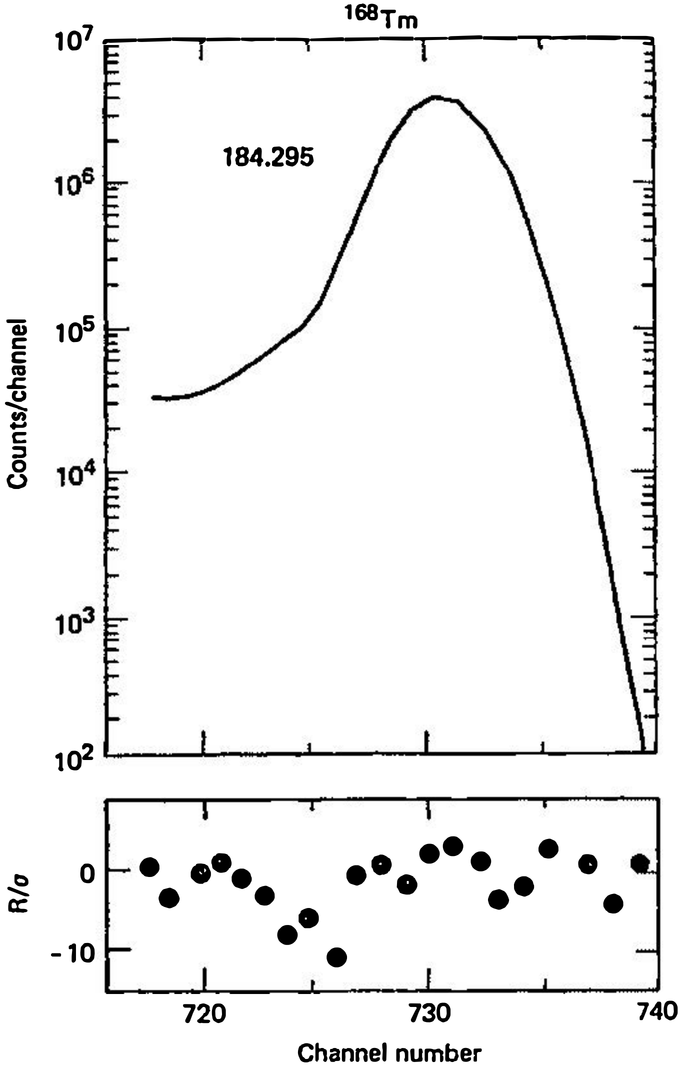

Fig. 3. GAMANAL peak shape fit to 184.295-keV photopeak of ^{168}Tm (note number events per channel exceeds 10^6, see text).

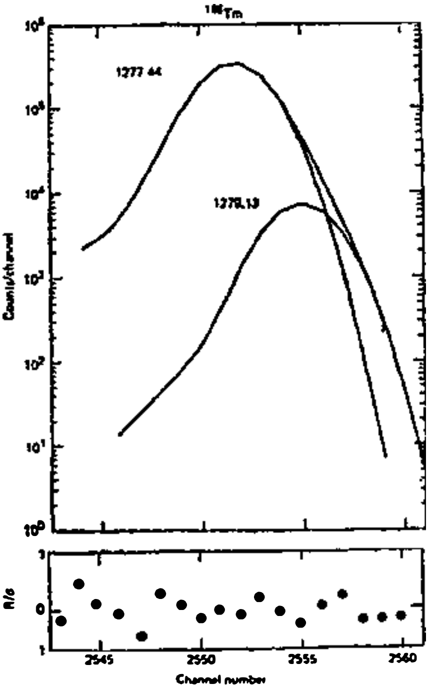

Fig. 4. GAMANAL peak shape fit to doublet with lower-energy lower-emission-rate component (^{168}Tm decay).

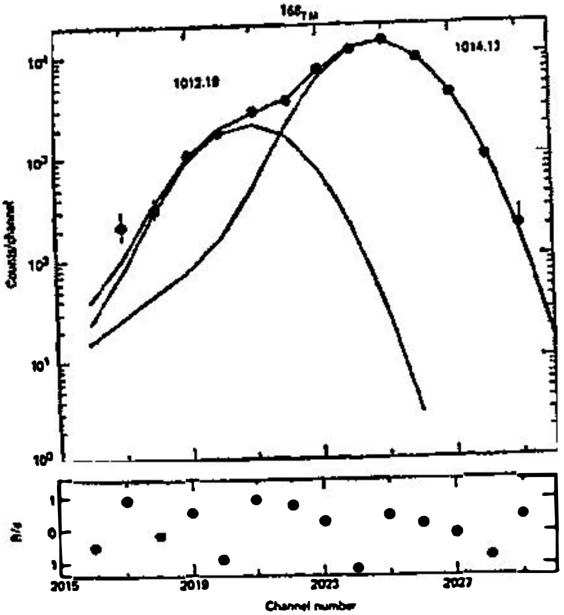

Fig. 5. GAMANAL peak shapc fit to doublet with higher-energy lower-emission-rate component (^{168}Tm decay).

3. *Efficiency determination*

If Ge (Li) detectors are to be used for quantitative measurements, they must be calibrated using appropriate sources. The counting efficiency at any particular γ-ray energy is dependent on a number of factors. Most of these are associated with the photon interaction process within the detector, the source-detector geometry, or with γ-ray attenuations within the source or from surrounding materials. If the samples to be analyzed all have the same size, shape, set of radioactive components, and activity level, then it is possible to carry out a specific calibration for this sample type such that γ-ray peak areas can be directly converted to the desired units. This condition does not generally prevail in our case. As a consequence, Gunnink has developed a more flexible approach in which he separates the overall efficiency into two components as follows: efficiency $= \varepsilon \times G$, where $\varepsilon =$ intrinsic efficiency, and $G =$ a geometry factor including attenuation factors. This scheme requires only one efficiency curve, which can be used for all samples without regard for their shape, size, activity level, or distance from the detector. A rather elaborate model has been developed to compute the geometry factor and has been discussed by Gunnink$^{12)}$. We have explored the question of how well we can fit a region of the efficiency curve above 300 keV but below 2000 keV. This was done as part of our studies of ^{134}Cs decay where special attention was given to the measurement of the relative γ-ray emission probabilities as precisely as possible. The uncertainties shown for the relative emission probabilities in the tables are a result of the measurements described by Van Hise$^{13)}$.

One might ask if there is a way one can test the relative efficiency curves that are in use today by using sources that have an inherent accuracy better than the known detector efficiencies. The answer is a qualified yes. First, we wish to recall some pertinent nuclear decay features. If the ground-state spin of a parent nucleus differs greatly from the ground-state spin of the decay product nucleus, then any decay branch occurring directly between the ground states is negligibly small. In this case, the decay may cascade through several levels where maximum angular momentum change occurs. In the ideal case, a γ-ray cascade will result with several γ-rays of with equal emission probabilities but different energy. We have encountered at least three cases, the decays of ^{93}Mo^{m}, ^{48}V and ^{48}Sc. In the decay of these three nuclei, their low nuclear charge Z does not allow significant electron conversion to occur. Our measurements can easily reproduce equal γ-ray emission probabilities for the γ-rays from three decays to within 2 percent. However, to reach the statistical accuracy of 0.3 percent, special attention has to be given not only to recalibration of the spectrometer but also the peak shape fit of each γ-ray peak.

We have re-examined the relative efficiency curves of a Ge (Li) and a high-purity Ge coaxial detector by using a combination of standard multigamma-ray sources and thermal-neutron-capture gamma rays$^{4)}$. Standard γ-ray sources have been used in the energy range up to approximately 3 MeV for both detectors. The thermal neutron capture on targets of stable chromium istopes and ^{35}Cl were used for producing γ rays up to approximately 10 MeV. The thermal-neutron-capture cross section for both targets is relatively high (σ_c (^{53}Cr) = 18 b; σ_c (^{35}Cl) = = 43 b), and prominent γ-rays of well known energies and emission probabilities are emitted$^{14-16)}$, which are well spaced over a wide energy range. These γ-rays are suitable for determinations of detector efficiency. In addition, both targets are easily accessible and have physical properties that are tractable. The common neutron capture standard, ^{14}N[14], is also a potential source of high energy calibration information, but was not used in this calibration because of its relatively low thermal-neutron-capture cross section. Relative emission probabilities of high-energy γ-rays such as $^{53}\mathrm{Cr}\,(\mathrm{n}, \gamma)\,^{54}\mathrm{Cr}$ and $^{14}\mathrm{N}\,(\mathrm{n}, \gamma)\,^{15}\mathrm{N}$ reactions were first determined using relative efficiency curves deduced from two γ-ray cascades from (p, γ) resonances[17].

The lack of consistent, reliable efficiency standards at high energy has caused many measurements of thermal-capture-gamma-ray emission probabilities to be in error by more than 10%. With experimental improvements the uncertainty of relative emission probabilities for γ-rays in the $^{35}\mathrm{Cl}\,(\mathrm{n}, \gamma)\,^{36}\mathrm{Cl}$ reaction have been reduced to a value which is comparable to those for the γ rays from the $^{14}\mathrm{N}\,(\mathrm{n}, \gamma)\,^{15}\mathrm{N}$ reaction ($\approx 5\%$). For our work, we have combined both standard multigamma-ray sources and capture γ-ray sources to determine the relative detector efficiency curve by normalizing strong low-energy γ-rays in the capture γ-ray sources to the curve determined from radioactive standards. If the γ-ray emission probability per decay of the standard γ-ray source is known, the intrinsic efficiency of the detector can also be determined at high energy.

An external beam of thermal neutrons with a flux of approximately $10^9\ \mathrm{n} \cdot \mathrm{cm}^{-2} \cdot \mathrm{s}^{-1}$ were obtained from the Livermore Pool-Type Reactor. Targets of natural abundance chromium metal and $\mathrm{CCl_4}$ sealed inside a pyrex tube were placed separately in the neutron beam at a distance of 32 cm from the leadshielded γ-ray detector. Liquid-nitrogen-cooled ORTEC coaxial detectors (one Ge (Li) and one high-purity Ge), both with an efficiency of approximately 13% and a resolution of approximately 2 keV at 1.332 MeV, were placed at an angle of 90° to the neutron beam. Standard nuclear spectroscopy equipment including a Canberra 80 series multichannel analyzer was used. A standard Pb X-ray absorber consisting of Cu and Cd foils surrounded the detector during the measurements. Extraction of γ-ray peak areas from the spectral data was done by using the available programs in the analyzer.

In Fig. 6 we present the relative efficiency curves for both detectors that result from our work using a combination of standard multigamma-ray sources and capture γ-rays. The top curve in Fig. 6 is for the high-purity Ge detector while the bottom curve is for the Ge (Li) detector. Both curves deviate rather rapidly from the straight line extrapolation above 3 MeV on the log-log graph. At approximately 10 MeV, the measured efficiency is approximately a factor of 2 below the efficiency obtained by a straight line extrapolation from lower energies. For the energy region between 300 keV and 3 MeV, the curve appears to be a straight line. The dotted lines indicate the linear extrapolations for the purpose of comparisons with the measured relative efficiency curves. These relative efficiency curves are similar in shape to those measured by McCallum and Coote[17].

Table 1 gives the coefficients of 5th and 6th order polynomials obtained from an unweighted computer fit to the data points for two different energy regions. The polynomials are in the form of $\ln \varepsilon_i = \sum_{j=1,6} a_j\,(\ln E_i)^{j-1}$, where E_i represents the γ-ray energy in units of MeV and a_j are coefficients given in Table 1. Both polynomials are plotted as smooth curves in Fig. 6.

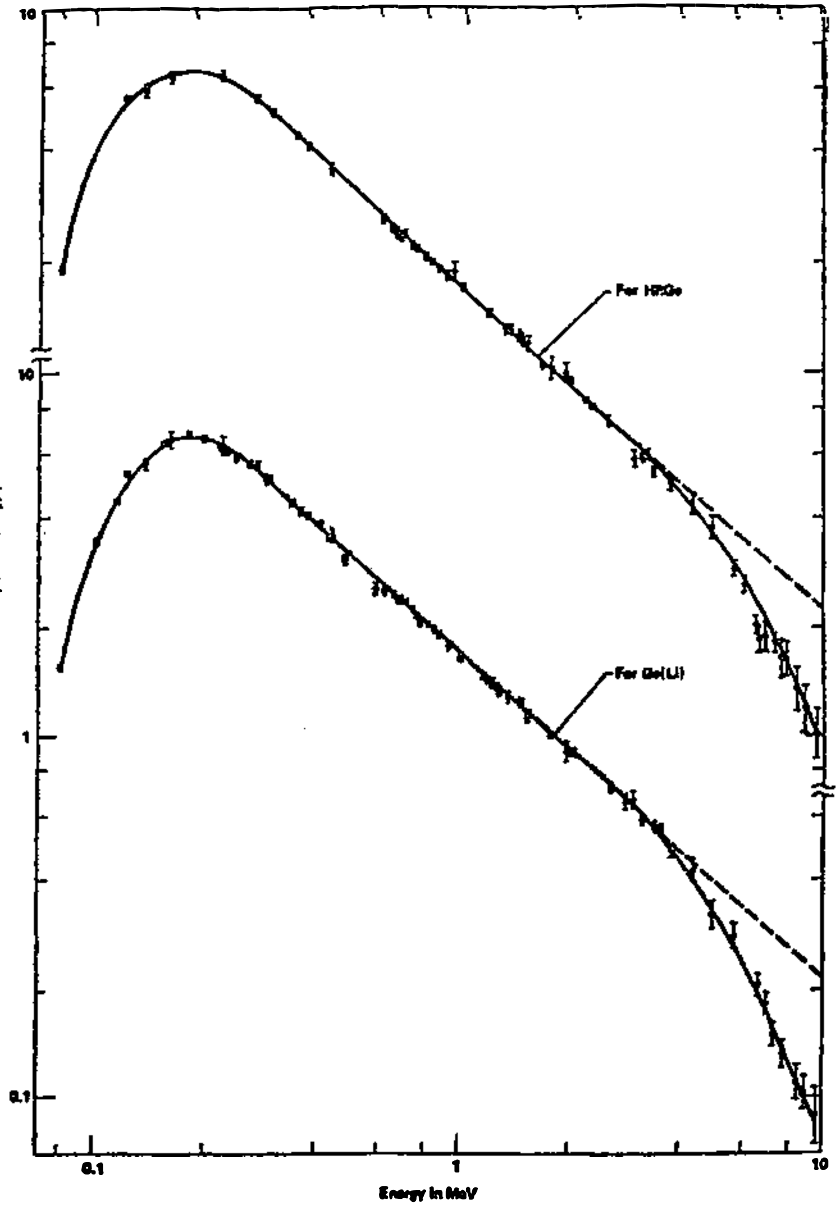

Fig. 6. Relative efficiency curves. The upper curve is for the high-purity Ge detector and the bottom one is for the Ge (Li) detector. Both detectors with X-ray absorbers were placed at 32 cm to the target.

When plotted on a semilogarithmic plot, the relative efficiency curve for each detector appears to be linear from 2 to 10 MeV. From the practical point of view,

TABLE 1.

	High-purity Ge with X-ray absorber		Ge(Li) with X-ray absorber	
	80 1,000 (keV)	700 10,000 (keV)	80 1,000 (keV)	700 10,000 (keV)
a_1	5.583484×10^{-1}	5.554820×10^{-1}	5.454347×10^{-1}	5.425167×10^{-1}
a_2	-8.143926×10^{-1}	-8.513116×10^{-1}	-8.200305×10^{-1}	-9.039662×10^{-1}
a_3	-4.716715×10^{-2}	-4.417474×10^{-2}	-8.378286×10^{-2}	1.493954×10^{-2}
a_4	-2.651750×10^{-1}	-3.969594×10^{-1}	-3.384564×10^{-1}	2.451231×10^{-1}
a_5	-1.457360×10^{-1}	2.453228×10^{-1}	-1.741303×10^{-1}	-2.886225×10^{-1}
a_6	0	-1.497862×10^{-2}	0	6.229418×10^{-2}

Coefficients of Polynomials for Relative Efficiency Curves $\ln \varepsilon_i = \sum_{j=1,6} a_j (\ln E_i)^{j-1}$.

TABLE 2.

E_γ (keV)	I_γ^a Previous[b]	Present work
460	0.97(2)	0.83(4)
610	—	1.68(4)
764	1.0(3)	2(6)
775	≡100.0(26)	≡100.0(3)
802	20.8(6)	20.5(5)
869	5.39(9)	5.28(6)
1053	2.07(7)	2.3(3)
1074	1.65(4)	2.8(1)
1147	—	0.95(7)
1352	1.05(10)	1.2(2)
1694	5.2(4)	4.0(3)
1855	1.66(8)	1.2(1)
2053	0.92(4)	0.8(1)
2215	0.83(5)	0.9(1)
2624	2.52(7)	2.6(2)
2875	2.52(9)	3.2(2)
2934	2.38(9)	2.9(2)
2946	3.12(10)	4.3(2)
3279	2.99(11)	3.8(3)
3933	5.38(15)	7.5(3)
4018	2.81(12)	3.3(3)
4721	1.45(5)	1.5(4)
6999.2(2)	0.28(3)	0.44(3)

Comparison between Present and Previously Reported Values for the Intensity of Major γ-Rays in the Decayed Fission Product of ^{88}Br.

[a] Relative intensity normalized to 100 for the 775-keV γ-ray.

[b] Taken from Ref. 23.

extension of the relative efficiency curve based on a straight line extrapolation on a semilogarithmic plot would be a workable method for obtaining an approximate relative efficiency curve at high energy, even without using thermal neutron capture γ-rays. Since the slope of the curves for these two detectors is slightly different at high energy, it would become more reliable to have at least one independent calibration point at high energy. A possible calibration point is the 6.129-MeV γ-ray that is emitted from a level of the same energy in ^{16}O. This γ-ray is emitted following the reaction $^{13}C(\alpha, n)^{16}O$. A combination source such as $^{244}Cm +$ $+ ^{13}C$ can be made and the emission rate for the 6.129 MeV γ-ray can be measured. Hence, a secondary standard γ-ray source for establishment of the high-energy portion for both energy and efficiency calibration is possible. A comparison between our new relative γ-ray emission probabilities for ^{88}Br decay which emit γ-rays with energies up to 7000 keV, is compared to previous values in Table 2.

We employed separate techniques to determine a set of γ-ray energy standards. These standards were then used in turn as »mixed standards« sources to determine the energy of the more intense γ-ray peaks of our multigamma-ray standards. The details of our techniques were presented in the ERDA workshop on γ-ray spectroscopy[1]. Here we repeat some of the considerations.

Cascade-Crossover Method: A fundamentally sound method for »bootstrapping« to higher energies involves summing the energies of cascade transitions to obtain the energy of the crossover transition after correcting for recoil energy difference. Some γ-ray cascades in the decay of ^{192}Ir have been used by Kessler et al.[18] to investigate small systematic energy-dependent uncertainties in their very precise series of γ-ray measurements.

In their work Greenwood, Helmer and Gehrke[19-21] used the two different sets of cascades as a basis for substantially increasing the number of γ-ray energy standards below 1300 keV and then extended γ-ray energy standards to 3.5 MeV[21]. The measured energy difference were obtained using Ge (Li) spectrometer techniques. The values obtained for energy differences are relatively insensitive to changes in the calibration energies. Explicit energy differences enable easier future revision in case more accurate primary standards become available. These authors have also done a more careful uncertainty analysis than one finds in much of the previous work. They explicitly identified the systematic uncertainty component of the fundamental energy values defining their energy scale. This uncertainty is clearly common to all γ-ray energies measured on this scale and must be identified in order that uncertainties may be properly combined. It is perhaps the lack of rigor in obtaining weighted averages and in using a basic scale intermediately between the two energy sets which resulted in the work in the above references being rejected by Kern.

Ge (Li) γ-Ray Energy Measurement Technique — Uncertainty Components: In a precision Ge (Li) γ-ray-energy measurement, data from an »unknown« source (source to be measured) and from a set of standard sources are accumulated simultaneously. Energy values for γ-rays in the unknown source are then obtained by comparison with those of standard γ-ray peaks in the spectrum.

System Nonlinearity: To limit the uncertainty due to system nonlinearity, the unknown full-energy peak should be relatively close to the standard peak to which it is being compared. A sufficient number of adequately well known standards should cover the energy region of interest to permit the nonlinearity function to be determined. Since the electric field effect produce nonlinearity[22], γ-rays from the unknown sources should enter the detector at the same range of angles as those from the standards and preferably in a perpendicular direction with respect to the source.

Good technique must be used in developing the nonlinearity curve and handling the associated uncertainties. In order to take into account the combined system nonlinearity, we fit by least-squares methods the energies of the standard γ-rays in each spectrum with a power series polynomial of the form: $E_i = \sum_{n=0}^{N} a_n \cdot C_i^n$ where E_i is the energy corresponding to the channel C_i. For each of the standard sources, γ-ray energies and centroids along with corresponding estimated standard deviations were input to a computer code. The appropriate standard deviation of the energies includes only measurement uncertainties, not the reference component to the total uncertainty. (Reference uncertainties bear a common relationship to all of the standards and, hence, should not affect the weighting). The code generates an error matrix which gives the total measurement uncertainties for any peak energy under consideration. This includes contributions due to the measurement uncertainty of the standard γ-ray energies, the peak fitting uncertainties, and an uncertainty associated with interpolating between standard γ-rays. (The size of the uncertainty envelope at a given energy depends on its proximity to the standards.) For most spectra, a polynomial of order 4 or 5 proved to be adequate to fit the standard γ-ray energies as a function of centroid channel with an average deviation of less than that of the average statistical deviation of the measurement of the standard γ-ray energies themselves. No apparent integral nonlinearity remained and the deviations from the fit suggest that differential nonlinearities are small.

Addition of Uncertainties in the Cascade-Crossover Method: A problem in using the cascade-crossover method which is not fully appreciated is the complexity in the uncertainty analysis. Because of the interdependence of uncertainties, a rigorous γ-ray energy uncertainty analysis, particularly when several cascades are involved, is very difficult. Consider a decay scheme for which we wish to determine the energy and uncertainty of the crossover γ-ray ($E_{\gamma 3} \pm \sigma_{\gamma 3}$) by measuring the energies of two cascade γ-rays (γ_1 and γ_2) with total uncertainties $\sigma_{\gamma 1}$ and $\sigma_{\gamma 2}$, respectively. Clearly

$$E_{\gamma 3} = E_{\gamma 1} + E_{\gamma 2} \, (+ \text{ recoil corrections}).$$

If the uncertainties in $E_{\gamma 1}$ and $E_{\gamma 2}$ are independent then

$$\sigma_{\gamma 3} = [\sigma_{\gamma 1}^2 + \sigma_{\gamma 2}^2]^{1/2}.$$

Using a 25 eV scale uncertainty combined with 10 eV measurement uncertainties for γ_1 and γ_2 (i. e., $E_{\gamma 1} \approx E_{\gamma 2} \approx 1$ MeV):

$$\sigma_{\gamma 3} = [(27)^2 + (27)^2]^{1/2} \text{ eV} = 38 \text{ eV}.$$

But can we assume that $\sigma_{\gamma 1}$ and $\sigma_{\gamma 2}$ are independent. Consider two cases:

Case 1: $E_{\gamma 1}$ and $E_{\gamma 2}$ are both determined by comparison with the same standard γ-ray — clearly the scale uncertainty σ_s is a systematic uncertainty component which must be separated out and added directly. Hence

$$\sigma_{S3} = \sqrt{\sigma_{S1}^2 + \sigma_{S2}^2} = 2\sigma_{S1}$$

$$\sigma_{M3} = [\sigma_{M1}^2 + \sigma_{M2}^2]^{1/2}$$

$$\sigma_{\gamma 3} = [\sigma_{M3}^2 + \sigma_S^2]^{1/2},$$

where σ_{mi} is the measurement uncertainty of the i^{th} γ-ray. For example:

$$\sigma_{\gamma 3} = [(10)^2 + (10)^2 + (50)^2]^{1/2}\ \text{eV} = 52\ \text{eV},$$

an increase of 27% over the result obtained by disregarding systematic components. If, however, γ_1 and γ_2 were compared to different standard lines, the effect would be less serious.

Case 2: Consider the same cascade with γ_1 and γ_2 each close in energy to a different standard γ-ray. Can we now treat the uncertainties in the two standard γ-ray energies as being independent, giving

$$\sigma_{S3} = [\sigma_{S1}^2 + \sigma_{S2}^2]^{1/2}.$$

We can only if σ_{S1} and σ_{S2} have no common elements. However, this is not usually the case. If the two calibrated γ-rays have a common »ancester« (a standard γ-ray) from which their energies were obtained, then the uncertainty in the ancestor is common to both and is therefore a systematic uncertainty. Once this common element is identified, then the uncertainty in each standard γ-ray energy is obtained from $\sigma_s = [\sigma_1^2 + \sigma_2^2]^{1/2}$, where

$\sigma_1 \equiv$ the systematic component of the uncertainty in the primary or secondary standard, and

$\sigma_2 \equiv$ the independent component of the uncertainty in the standard.

The total uncertainty due to the standards becomes

$$\sigma_{S3} = [\sigma_1^2 + \sigma_2^2 + (\sigma_1 + \sigma_2)^2]^{1/2}.$$

Based on Helmer and coworkers, it is reasonable to assume that of the 25 eV uncertainty in the standard γ-ray energies, the systematic component is at least 21 eV. Using this value along with other uncertainties used in Case 1 gives

$$\sigma_{S3} = [(14)^2 + (14)^2 + (42)^2]^{1/2}\ \text{eV} = 46\ \text{eV},$$

and for the total uncertainty in the crossover γ-ray

$$\sigma_{\gamma 3} = [(10)^2 + (10)^2 + (46)^2]^{1/2}\ \text{eV} = 48\ \text{eV},$$

which is still substantially higher than the 38 eV obtained when systematic uncertainty components were disregarded. Of course, the effect of incorrectly handling systematic uncertainties decreases rapidly with increasing measurement uncertainties. However, the effect also increases with γ-ray energy since the uncertainty in the standard γ-ray energies is dominated by the systematic component above about 1 MeV.

The least-squares fitting procedures frequently used to obtain adjusted energies must be critically examined. Because of the interdependence of the uncertainties in the γ-ray energies involved, it is not clear that the proper weights are used for the least-squares procedure. The uncertainty in the average level energy may be too small because the assumptions concerning the input uncertainties are not valid. What is needed and certainly does not now exist, is a procedure for obtaining level energies in which the uncertainties are handled rigorously.

Gamma-Rays in the 1.2 *to* 1.8 *MeV Energy Range*: As an example of the use of the cascade-crossover method to calibrate higher-energy γ-rays, we will discuss the measurements made in the 1.2 to 1.8 MeV energy range. The radioactive isotopes ^{72}Ga, ^{82}Sr, ^{110m}Ag and ^{124}Sb were used simultaneously for this range because they provide many cascade-crossover combinations. As can be seen from Table 3, there is a good distribution of crossover γ-ray energies with which to define a nonlinearity curve. Note that we have tabulated the uncertainties due to the standard γ-rays at 411 keV and 675 keV separately to aid in the calculation of total crossover γ-ray uncertainties. These intermediate energy crossover rays serve as secondary standards for the direct comparison with cascade γ-rays from the decay of ^{72}Ga, ^{56}Co and ^{56}Mn which enable us to extend the calibration to 3.5 MeV2).

TABLE 3.

Isotope	Crossover (keV)	Measure	675[a]	411[a]	Total	Cascade γ-rays
Br-82	1317.473	5	8	16	19	619+698 827+1043−544
Ag-110m	1384.305	8	8	17	20	677+706 620+763 446+937
Ga-72	1464.084	11	8	18	23	629+834
Ag-110m	1505.039	8	16	18	25	620+884 686+818
Ag-110m	1562.305	11	16	19	27	744+818 677+884
Ga-72	1596.744	11	16	19	27	786+810
Sb-124	1690.992	10	16	20	27	645+1045

Gamma-ray Cascade and Crossover Transitions used in the 1.2 to 1.8 MeV (Uncertainty Components in eV).

[a] Uncertainty due to standard γ-rays at 675 and 411 keV.

4. *Table of multigamma-ray source values and intercomparison*

In the appendix we present our current γ-ray energies and emission probability values for a number of standards. Some of these have been compared to other values in the literature[6–7]. As discussed earlier our values for ^{152}Eu compare well with the ICRM intercalibration efforts (see Table 4). It should be noted that the γ-ray energy values are determined independently of the work of Helmer and coworkers. Hence, they provide an independent check on those values published after our original work (e. g. see Ref. 21) (see Table 5).

TABLE 4.

E_γ	LLNL	ICRM
112[a]	1362(16)	1361(11)
245	358(6)	360(3)
344	1275(9)	1275(8)
411	107(1)	107(1)
444	148(2)	150(1)
779	619(8)	622(3)
964	692(9)	701(2)
1086[b]	487(2)	487(2)
1112	649(9)	650(2)
1408	1000(3)[c]	1000(3)

Comparison of ^{152}Eu γ-ray emission-probability values.

[a] For nonmass-separated sources, ^{154}Eu can contribute to the observed emission probability of a 122-keV line.

[b] In our work, this line is a resolved doublet of 1084- and 1085-keV with relative emission probabilities of 11.7 and 475, respectively.

[c] Fiducial. This represents a peak-fitting uncertainty only.

TABLE 5.

LLNL E_γ (ΔE_γ)	Ref. 20 E_γ (ΔE_γ)
846.772(8)	846.764(6)
1037.840(6)	1037.844(4)
1175.102(6)	1175.099(8)
1238.282(7)	1238.287(6)
1360.215(12)	1360.206(6)
1771.351(16)	1771.350(15)
2015.181(16)	2015.179(11)
2034.755(15)	2034.759(11)
2598.458(13)	2598.460(10)
3009.591(22)	3009.596(17)
3201.962(16)	3201.954(14)
3253.416(15)	3253.417(14)
3272.990(15)	3272.998(14)
3451.152(17)	3451.154(13)
3547.925(61)	

Comparison for γ-ray Energies of ^{56}Co in keV.

TABLE 5A.

LLNL E_γ (ΔE_γ)	Ref. 24 E_γ (ΔE_γ)
446.808(8)	446.815(4)
620.362(1)	620.359(3)
657.766(5)	657.761(2)
677.623(7)	677.625(4)
687.005(11)	687.012(4)
706.688(8)	706.678(5)
744.279(8)	744.278(5)
763.947(8)	763.944(4)
818.037(8)	818.029(5)
884.689(8)	884.682(5)
937.502(13)	937.488(5)
1384.305(8)	1384.299(4)
1475.305(12)	1475.785(5)
1505.039(8)	1505.036(5)
1562.305(9)	1562.301(6)

Comparison of γ-ray Energies for ^{110}Ag^{m} in keV.

TABLE 6.

	I_γ (ΔI_γ) in γ-rays/100 decays				
E_γ (keV)	88 cm	21.7 cm	16.7 cm	1.3 cm	Ratio emission probability 1.30 cm/88 cm (% of 88 cm) (value)
79	10.86(5)	10.5(1)	10.4(3)	12.4(1.2)	114
99	4.20(2)	4.28(3)	4.2(2)	4.2(1)	100
184	17.4(2)	17.6(2)	17.5(5)	14.5(3)	83
198	52.2(5)	53.1(5)	52.8(5)	45.6(3)	87
348	0.34(1)	0.35(2)	0.39(4)	0.26(1)	76
422	0.29(1)	0.30(2)	0.34(4)	0.23(2)	79
447	23.0(1)	22.6(4)	22.7(3)	18.0(2)	78
547	2.54(2)	2.53(2)	2.53(5)	2.25(5)	89
631	8.84(5)	8.71(11)	8.81(11)	7.20(9)	81
645	1.45(1)	1.49(4)	1.5(5)	2.69(5)	186
720	11.90(5)	11.80(11)	11.9(1)	11.2(1)	94
731	5.05(2)	5.00(11)	5.0(1)	4.38(5)	87
741	12.27(5)	12.27(11)	12.5(1)	12.17(9)	99.2
748	0.41(1)	0.42(2)	0.41(5)	0.39(2)	95
816	48.8(2)	48.7(7)	49.0(3)	43.8(3)	90
821	11.48(5)	11.48(21)	11.48(11)	11.58(9)	100.9
830	6.68(5)	6.75(11)	6.76(5)	6.88(9)	103
915	2.99(2)	2.98(5)	3.01(5)	3.16(3)	106
1277	1.61(1)	1.64(3)	1.67(5)	1.74(2)	108
1461	0.24(1)	0.24(2)	0.25(3)	0.74(2)	308

Comparison of the More Abundant γ-Rays from the Decay of ^{168}Tm with Source Detector Distances from 88 cm to 1.7 cm.

5. Counting geometry

A number of multigamma-ray sources must be used only at large (>10 cm) counting distances. A good example of this is the γ-ray metrology of ^{168}Tm which often involves the measurement of low-activity sources. The measurement of these low-activity sources, in turn, requires that small source-to-Ge (Li) detector distances be used. In such cases the reliance on γ-ray emission probabilities per decay may lead to incorrect results. For ^{168}Tm decay, a majority of the transitions occur in such a way that severe summing can occur. This is illustrated in Table 6 where we compare the measurement of ^{168}Tm at several different source-to-detector distances. As can be seen in the last column in Table 6, only three γ-rays exhibit constant emission probabilities when the value for the 1.3-cm counting distance is compared to the 88-cm counting distance. Those are the 99-, 741- and 821-keV γ-rays. The slight variation of the emission probabilities for the 741- and 821-keV γ-rays may be real since the 741-keV γ-ray can sum with the 79-keV γ-ray to produce an 821-keV event. Thus, the slight diminishing of the 741-keV γ-ray emission probability shows up in the 821-keV γ-ray. In general, we find that because of these effects and other counting effects, it is appropriate to calibrate the entire system of sample configuration, source-to-detector distance, and Ge (Li) detector efficiency for each measurement if precise results are required.

Appendix

^{44}Sc^{m+g} (58.6h and 3.93h; from 47y ^{44}Ti)

$E_\gamma\,(\Delta E_\gamma)$	$I_\gamma\,(\Delta I_\gamma)$
271.248(10)	778(14)
1001.850(31)	12.3(1)
1126.092(40)	12.3(1)
1157.031(15)	1000(3)
1499.489(25)	9.0(2)
2144.3(1)	0.02(2)[b]
2150.840(22)[a]	0.011(3)
2656.478(30)	1.11(4)
3301.3(1)	0.0064(8)

---

[a] The γ-ray energy is from ^{44}K decay.

[b] Interference from the natural background precluded obtaining a precise value.

^{48}Sc (43.8h)

$E_\gamma\,(\Delta E_\gamma)$	$I_\gamma\,(\Delta I_\gamma)$
175.361(5)	74.7(9)
983.526(12)	1000(3)
1037.522(12)	975(5)
1212.880(12)	23.8(4)
1312.120(12)	1000(5)

^{48}V (16.21d)

$E_\gamma\,(\Delta E_\gamma)$	$I_\gamma\,(\Delta I_\gamma)$
803.25(8)	1.5(2)
928.327(9)	7.7(5)
944.125(7)	77.6(9)
983.526(5)	1000(2)
1063.9(1)	0.05(1)
1312.090(12)	975(8)
1437.35(7)	1.2(2)
2240.398(10)	24.1(4)
2375.1(5)	0.10(5)
2421.8(5)	0.10(5)

^{28}Mg (21.0h) and ^{28}Al (2.24m)

$E_\gamma\,(\Delta E_\gamma)$	$I_\gamma\,(\Delta E_\gamma)$
30.641(20)	655(50)
400.700(21)	363(4)
607.1(5)	0.1(1)
647.9(2)	0.9(2)
941.474(32)	378(6)
982.9(5)	0.1(1)
1013.5(5)	0.1(1)
1342.284(32)	534(16)
1372.925(61)	48(2)
1589.400(33)	42(2)
1620.04(15)	3(1)
1778.895(34)	1000(30)

^{52}Fe (8.28h)

$E_\gamma (\Delta E_\gamma)$	$I_\gamma (\Delta I_\gamma)$
168.688(2)	1032(20)
377.748(5)	17.1(2)
704.6(2)	0.3(1)
1039.928(17)	0.99(4)
1434.092(17)	1000(5)
1530.709(19)	0.47(2)
1727.574(75)	2.2(1)

^{52}Mn (5.59d)

$E_\gamma (\Delta E_\gamma)$	$I_\gamma (\Delta E_\gamma)$
200.582(41)	0.76(2)
346.02(4)	9.8(1)
398.09(9)	0.89(7)
399.57(5)	1.83(7)
502.06(5)	2.1(2)
600.16(5)	3.9(1)
647.47(6)	4.0(2)
744.233(13)	900(8)
848.18(5)	33.2(3)
901.89(18)	0.44(4)
935.544(12)	945(9)
1045.746(80)	0.7(2)
1246.278(15)	42.1(6)
1247.88(9)	3.8(4)
1333.649(17)	50.7(5)
1434.092(17)	1000(5)
1645.822(36)	0.47(3)
1839.14(17)	0.05(1)
1981.120(38)	0.34(3)
2257.42(19)	0.027(6)

^{56}Co (78.5d)

$E_\gamma (\Delta E_\gamma)$	$I_\gamma (\Delta E_\gamma)$
263.41(10)	22(4)
411.38(8)	25(5)
486.54(11)	55(5)
733.72(15)	200(10)
787.88(7)	310(10)
846.772(8)	100,000
896.56(20)	70(5)
977.485(60)	1,440(15)
997.33(16)	112(6)
1037.840(6)	14,000(100)
1089.03(24)	50(10)
1140.28(10)	150(10)
1160.08(16)	100(10)
1175.102(6)	2,280(20)
1198.78(20)	50(10)
1238.282(7)	67,600(400)
1272.2(6)	20(2)
1335.56(8)	125(5)
1360.215(12)	4,330(40)
1442.75(8)	200(10)
1462.34(12)	77(5)
1640.54(13)	60(10)
1771.351(16)	15,700(150)
1810.714(35)	640(10)
1963.990(60)	720(15)
2015.181(16)	3,080(30)
2034.755(15)	7,890(70)
2113.185(115)	385(5)
2212.96(15)	350(10)
2276.36(16)	110(5)
2373.71(40)	80(10)
2523.86(20)	60(5)
2598.458(13)	17,290(150)
3009.591(22)	1,050(10)
3201.962(16)	3,240(30)
3253.416(15)	7,937(65)
3272.990(15)	1,890(20)
3369.69(30)	11(2)
3451.152(17)	954(10)
3547.925(61)	198(5)
3600.69(40)	18(1)

^{67}Ga (78.3h)

$E_\gamma (\Delta E_\gamma)$	$I_\gamma (\Delta E_\gamma)$
91.237(35)	30(2)
93.291(30)	366(14)
184.569(30)	217(9)
208.970(30)	24(1)
300.230(25)	166(4)
393.539(25)	45(1)
494.132(30)	0.7(1)
703.078(50)	0.10(1)
794.378(50)	0.53(3)
887.664(40)	1.49(5)

^{75}Se (120d)

$E_\gamma (\Delta E_\gamma)$	$I_\gamma (\Delta E_\gamma)$
24.391(55)	0.46(4)
66.061(6)	18.7(1)
80.937(30)	0.19(4)
96.734(3)	57.2(21)
121.121(4)	298.(2)
135.999(2)	1000(3)
198.596(8)	25.4(2)
264.658(3)	1000(5)
279.535(5)	422(4)
303.923(5)	22.3(2)
400.657(2)	195(3)
419.302(45)	0.18(3)
572.724(20)	0.60(3)
617.896(35)	0.077(4)
821.916(35)	0.0022(2)

^{82}Br (35.30h)

E_γ (ΔE_γ)	I_γ (ΔE_γ)
92.190(16)	9.0(3)
100.890(70)	0.84(8)
129.29(10)	0.36(7)
137.40(5)	1.8(2)
179.8(2)	0.12(9)
221.459(25)	27.2(8)
273.480(9)	10.0(5)
280.7(2)	0.15(4)
332.897(31)	1.08(5)
401.16(6)	1.09(9)
470.29(9)	0.6(2)
554.353(7)	848(16)
559.5(3)	0.16(9)
606.9(3620)	14.5(4)
619.111(7)	516(5)
698.368(8)	343(9)
735.637(55)	0.9(1)
776.516(4)	1000
827.831(6)	287(7)
932.1(2)	0.12(5)
952.017(30)	4.4(2)
1007.593(25)	15.7(4)
1044.077(6)	328(5)
1072.60(10)	0.95(15)
1081.290(50)	7.4(4)
1174.0(4)	0.21(7)
1180.1(2)	1.1(1)
1317.473(8)	322(6)
1426.0(1)	1.3(5)
1474.876(10)	1.99(3)
1650.365(40)	9.5(1)
1779.660(29)	1.4(2)
1956.6(1)	0.4(1)

^{83}Rb (83d)

E_γ (ΔE_γ)	I_γ (ΔE_γ)
9.390(90)	131(30)
32.181(50)	0.8(1)
119.323(90)	0.32(5)
128.55(12)	0.030(5)
520.423(25)	1000(5)
529.653(11)	656(30)
552.664(21)	357(15)
562.174(70)	0.19(2)
648.976(50)	1.9(1)
681.187(65)	0.7(1)
790.160(35)	14.7(4)
799.380(51)	5.3(2)

^{95}Zr (64.0d)

E_γ (ΔE_γ)	I_γ (ΔE_γ)[a]
235.696(20)	0.24(1)
724.202(12)	43.7(8)
756.734(15)	55.4(1.1)

[a] The values quoted are the emission probability per 100 decays.

^{105}Ag (41.0d)

E_γ (ΔE_γ)	I_γ (ΔI_γ)
38.771(70)	0.13(2)
64.072(70)	268(5)
90.012(70)	0.8(1)
112.51(5)	0.84(6)
155.38(5)	9.8(2)
159.00(8)	0.75(9)
182.92(3)	8.6(2)
202.21(9)	0.9(2)
216.1(2)	0.33(7)
270.5(2)	0.3(1)
280.54(2)	744(4)
284.8(1)	2.3(5)
289.38(8)	2.9(2)
306.30(4)	18.3(3)
311.75(4)	1.9(1)
319.24(1)	106(1)
325.44(5)	4.8(1)
328.62(5)	4.9(2)
331.59(2)	98.6(6)
344.61(1)	1000(3)
353.8(3)	0.2(1)
360.73(3)	11.3(2)
370.29(3)	17.6(2)
392.74(2)	47.8(4)
401.76(4)	4.6(1)
408.09(8)	1.0(2)
414.86(5)	7.2(2)
421.04(6)	2.9(1)
437.31(4)	6.9(2)
443.45(1)	259(2)
446.8(1)	2.4(2)
527.35(8)	2.6(2)
560.80(8)	13.5(1)
576.7(2)	0.6(1)
610.0(3)	0.2(1)
617.92(4)	28.6(3)
640.5(2)	0.7(2)
644.65(3)	242(2)
650.80(4)	60.0(6)
673.26(5)	23.3(4)
681.96(9)	1.8(4)
709.8(3)	0.16(8)
727.29(9)	3.5(1)
743.47(8)	12.7(3)

^{105}Ag (41.0d) continued.

$E_\gamma(\Delta E_\gamma)$	$I_\gamma(\Delta E_\gamma)$
768.9(3)	0.24(8)
807.59(5)	27.5(6)
844.6(2)	0.6(1)
921.2(2)	0.4(1)
929.2(2)	0.33(8)
962.47(9)	2.7(1)
1088.08(4)	86(1)
1125.3(3)	0.27(5)

^{108}Ag^{m} (130y)

$E_\gamma(\Delta E_\gamma)$	$I_\gamma(\Delta I_\gamma)$
433.939(4)	991(3)
614.281(6)	997(3)
633.012(38)	1.51(8)
722.938(8)	1000(3)

^{110}Ag^{m} (252d)

$E_\gamma(\Delta E_\gamma)$	$I_\gamma(\Delta I_\gamma)$
116.485(46)	0.085(3)
120.226(26)	0.19(1)
133.333(7)	0.77(3)
219.348(8)	0.70(2)
221.079(10)	0.72(1)
229.423(23)	0.128(8)
264.254(58)	0.059(5)
266.913(12)	0.43(1)
341.2(2)	0.022(4)
356.43(10)	0.045(4)
360.228(75)	0.035(7)
365.450(11)	1.02(8)
387.075(9)	0.55(1)
396.897(23)	0.43(1)
409.330(45)	0.068(7)
446.808(8)	38.9(6)
467.029(36)	0.26(5)
493.432(91)	0.11(1)
544.555(45)	0.22(1)
573.0(4)	0.13(3)
603.065(90)	0.042(9)
620.362(10)	29.4(5)
626.262(10)	2.48(4)
630.626(55)	0.40(1)
657.766(5)	1000
676.58(10)	1.5(1)
677.623(7)	112(2)
687.005(11)	68.3(5)
706.688(8)	172.8(5)
708.133(20)	2.9(2)

^{110}Ag^{m} (252d) continued.

$E_\gamma(\Delta E_\gamma)$	$I_\gamma(\Delta I_\gamma)$
744.279(8)	49.3(8)
763.947(8)	236(3)
774.8(2)	0.02(1)
818.037(8)	77.1(5)
884.689(8)	771(10)
937.502(13)	363(6)
957.368(85)	0.08(1)
997.258(15)	1.32(4)
1018.893(50)	0.15(1)
1085.462(14)	0.71(2)
1117.474(28)	0.52(1)
1125.714(20)	0.30(2)
1163.159(75)	0.79(7)
1164.959(85)	0.50(5)
1186.7(2)	0.015(5)
1251.057(42)	0.26(1)
1300.03(12)	0.21(1)
1334.341(17)	1.49(5)
1384.305(8)	261(5)
1420.081(50)	0.24(2)
1475.796(12)	42.4(8)
1505.039(8)	140.1(1.9)
1562.305(9)	12.6(6)
1572.4(2)	0.012(3)
1592.672(95)	0.22(1)
1629.692(63)	0.046(5)
1775.422(39)	0.063(4)
1783.480(30)	0.092(3)
1903.530(35)	0.16(1)
2004.74(10)	0.011(2)

^{90}Nb (14.6h)

$E_\gamma(\Delta E_\gamma)$	$I_\gamma(\Delta I_\gamma)$
132.716(18)	50.4(5)
141.178(15)	814(8)
329.058(16)	1.50(5)
337.50(15)	0.3(1)
371.307(8)	22.0(8)
420.280(50)	0.33(3)
425.5(2)	0.06(1)
518.597(58)	8.4(6)
561.604(11)	1.46(4)
757.949(44)	0.49(5)
792.05(19)	0.13(4)
827.744(36)	13.5(2)
890.644(41)	22.0(5)
1051.532(33)	2.6(1)
1057.8(1)	0.21(6)
1093.144(82)	1.2(1)
1129.224(15)	1130(5)
1192.7(1)	0.20(2)
1270.396(18)	15.8(3)

^{90}Nb (14.6h) continued.

$E_\gamma (\Delta E_\gamma)$	$I_\gamma (\Delta E_\gamma)$
1470.528(24)	5.6(2)
1575.035(23)	6.3(2)
1611.761(30)	29.0(8)
1658.097(31)	4.08(18)
1716.266(26)	6.1(2)
1843.342(22)	8.4(2)
1913.194(25)	15.6(2)
1984.535(28)	8.3(3)
2000.18(29)	0.8(1)
2056.095(75)	1.4(1)
2186.242(25)	219(2)
2222.343(28)	7.6(3)
2318.959(25)	1000(2)
2321.9(2)	9(2)
2741.0(3)	0.09(3)
2747.8(3)	0.06(2)

^{96}Mo (23.35h)

$E_\gamma (\Delta E_\gamma)$	$I_\gamma (\Delta I_\gamma)$
108.95(11)	0.46(15)
219.081(18)	30.8(5)
241.377(15)	40.0(7)
314.337(71)	0.77(14)
316.271(87)	0.63(9)
350.053(19)	16.0(4)
352.555(28)	8.6(4)
371.807(15)	27.2(9)
434.730(37)	3.9(3)
460.040(12)	276(2)
480.705(17)	60.5(5)
568.871(12)	601(3)
591.243(48)	9.7(9)
719.562(17)	71.0(9)
721.629(19)	10.6(6)
778.224(15)	1000(2)
810.330(15)	115(1)
812.581(15)	30.6(8)
847.687(22)	11.8(6)
849.929(13)	212(2)
1019.611(28)	2.1(1)
1052.57(11)	0.63(12)
1091.349(12)	5.1(1.5)
1126.965(21)	4.4(2)
1149.847(96)	0.54(11)
1200.231(13)	207(1)
1368.79(12)	0.43(9)
1497.807(15)	34.0(7)
1441.129(24)	4.6(2)
1588.377(28)	2.6(1)
1625.903(47)	1.6(1)
1627.803(22)	3.9(1)
1807.80(10)	0.59(8)
1869.207(58)	11(1)
1978.191(71)	3.8(3)

^{99}Mo (66.2h)

$E_\gamma (\Delta E_\gamma)$	$I_\gamma (\Delta E_\gamma)$
40.587(15)	103(5)
89.4(2)	0.3(2)
140.466(15)	9062(180)
142.675(25)	2.27(7)
158.782(15)	1.67(8)
162.370(15)	1.16(5)
181.057(15)	604(12)
242.286(76)	0.14(2)
249.030(27)	0.29(3)
366.421(15)	119(3)
380.133(79)	0.90(3)
410.274(95)	0.19(4)
411.491(15)	1.44(6)
455.84(13)	0.13(6)
457.603(29)	0.67(5)
469.629(70)	0.26(5)
490.53(15)	0.11(4)
528.788(15)	5.36(11)
537.79(15)	0.16(6)
580.505(65)	0.43(5)
581.30(12)	0.10(5)
620.026(35)	0.23(8)
621.771(24)	2.56(8)
739.500(17)	1200(33)
761.774(76)	0.11(1)
777.921(20)	424(9)
822.972(15)	12.7(4)
960.754(20)	9.1(2)
986.443(35)	0.13(1)
1001.343(18)	0.40(1)
1056.197(49)	0.10(1)

^{103}Ru (39.35d)

$E_\gamma (\Delta E_\gamma)$	$I_\gamma (\Delta E_\gamma)$
39.731(50)	0.79(5)
42.631(41)	0.012(2)
53.291(10)	4.2(2)

^{103}Ru (39.35d)

$E_\gamma (\Delta E_\gamma)$	$I_\gamma (\Delta E_\gamma)$
113.253(70)	0.040(8)
114.973(22)	0.089(8)
241.886(52)	0.17(2)
292.7(2)	0.03(3)
294.987(27)	2.80(9)
317.8(2)	0.06(1)
357.399(140)	0.10(3)
443.811(20)	3.6(11)
497.813(19)	1000(5)

^{103}Ru (39.35d) continued.

$E_\gamma (\Delta E_\gamma)$	$I_\gamma (\Delta E_\gamma)$
514.60(15)	0.054(15)
554.054(17)	9.3(3)
567.88(13)	0.018(8)
610.345(22)	63(2)
612.035(31)	0.9(1)
651.8(4)	0.0019(8)

^{113}Sn (115d)

$E_\gamma (\Delta E_\gamma)$	$I_\gamma (\Delta I_\gamma)$
255.066(50)	28.5(7)
391.698(15)	1000(3)
638.046(75)	0.0149(5)
646.8(1)	0.00006(3)

^{121}Te^{m} (150d)

$E_\gamma (\Delta E_\gamma)$	$I_\gamma (\Delta I_\gamma)$
37.139(2)	13.3(13)
65.550(7)	3.2(1)
81.790(15)	0.61(3)
103.853(78)	0.04(4)
212.194(27)	1039(18)
470.484(8)	17.5(3)
507.604(5)	220(3)
573.153(4)	1000(5)
909.870(15)	0.88(1)
947.013(15)	0.103(2)
998.316(5)	1.00(2)
1024.0(3)	0.0010(5)
1035.426(95)	0.007(3)
1102.177(15)	31.8(4)
1107.6(2)	0.005(2)
1144.679(35)	0.0135(5)

^{124}Sb (60.20d)

$E_\gamma (\Delta E_\gamma)$	$I_\gamma (\Delta I_\gamma)$
400.010(60)	1.5(1)
443.961(50)	2.0(1)
525.410(50)	1.6(1)
602.728(5)	1000(3)
632.386(45)	1.0(1)
645.858(6)	75.5(5)
709.320(13)	13.8(2)
713.793(6)	23.2(3)
722.789(6)	110(2)
735.738(26)	1.4(1)
790.727(16)	7.6(1)
968.208(7)	19.3(3)
976.23(11)	0.9(1)
1045.138(20)	18.8(4)
1325.516(8)	16.6(4)

^{124}Sb (60.20d) continued.

$E_\gamma (\Delta E_\gamma)$	$I_\gamma (\Delta E_\gamma)$
1355.175(22)	10.6(4)
1368.179(30)	26.8(5)
1376.112(45)	5.1(4)
1436.577(12)	12.6(5)
1445.058(39)	3.4(4)
1488.886(24)	7.1(3)
1526.177(47)	4.1(3)
1579.778(47)	4.2(3)
1690.992(16)	484(8)
1919.82(20)	0.5(1)
2039.299(30)	0.7(1)
2090.962(35)	57(1)
2099.10(10)	0.4(1)
2108.080(80)	0.4(1)
2182.610(90)	0.4(1)
2283.30(10)	0.08(1)
2293.710(40)	0.31(1)
2323.1(3)	0.024(2)
2454.4(4)	0.007(3)
2682.0(4)	0.016(2)
2693.680(60)	0.026(3)

^{125}Sb (2.73y)

$E_\gamma (\Delta E_\gamma)$	$I_\gamma (\Delta E_\gamma)$
110.895(12)	0.009(1)
116.955(11)	2.55(4)
146.08(10)	0.0062(4)
172.619(15)	1.82(3)
176.388(4)	67.9(2)
178.785(50)	0.27(4)
198.655(60)	0.13(3)
204.134(25)	3.23(4)
208.093(25)	2.36(4)
227.917(35)	1.32(4)
314.95(11)	0.042(4)
321.04(4)	4.10(4)
380.445(20)	15.2(1)
408.02(4)	1.83(6)
427.900(15)	294(2)
443.508(35)	3.03(7)
463.395(15)	104.5(1.5)
497.37(12)	0.036(4)
600.572(18)	177.8(2.0)
606.656(19)	50.2(7)
635.911(18)	113.2(1.8)
671.426(20)	18.0(4)

^{126}I (13.0d)

$E_\gamma (\Delta E_\gamma)$	$I_\gamma (\Delta E_\gamma)$
388.643(5)	1030(5)
491.255(4)	86.1(3)
666.348(6)	1000(3)
695.0(1)	0.007(3)

^{126}I (13.0d) continued.

E_γ (ΔE_γ)	I_γ (ΔI_γ)
753.838(7)	125.8(6)
879.898(8)	22.8(6)
1206.8(3)	0.014(4)
1420.23(3)	8.91(5)
2045.14(5)	0.14(1)

^{131}I (8.041d)

E_γ (ΔE_γ)	I_γ (ΔE_γ)
80.185(2)	26.0(3)
85.9(2)	0.0009(5)
177.214(2)	2.63(2)
232.18(15)	0.014(18)
272.498(17)	0.56(1)
284.305(5)	60.1(6)
295.8(2)	0.007(4)
302.4(2)	0.05(1)
318.088(16)	0.79(3)
324.651(25)	0.22(4)
325.789(4)	2.49(4)
358.4(2)	0.091(2)
364.489(5)	806(16)
404.814(4)	0.56(2)
449.6(2)	0.07(2)
503.004(4)	3.58(7)
636.989(4)	72.1(9)
642.719(5)	2.18(4)
722.911(5)	17.9(4)

^{131}Ba (11.7d)

E_γ (ΔE_γ)	I_γ (ΔI_γ)[a]
54.877(25)	2.8(9)
78.761(18)	24(1)
82.481(35)	0.5(2)
92.287(15)	20.8(7)
123.831(12)	1000(5)
133.638(12)	76.3(1.5)
137.386(18)	1.3(1)
157.187(15)	6.9(2)
216.118(12)	689(20)
239.635(13)	93(9)
246.919(15)	21(1)
249.432(15)	98(4)
294.489(15)	5.5(7)
351.211(17)	3.4(5)
373.245(15)	478(25)
404.043(15)	46(2)
461.266(19)	4.0(2)

^{131}Ba (11.7d) continued.

E_γ (ΔE_γ)	I_γ (ΔE_γ)
480.416(14)	11.7(5)
486.523(15)	73(1)
496.330(15)	1612(35)
534.15(10)	0.26(5)
572.720(15)	10.5(8)
585.058(14)	45(3)
620.165(18)	51(3)
674.479(25)	4.7(4)
696.552(15)	6.0(4)
703.40(10)	0.3(1)
831.615(35)	8.5(5)
914.119(25)	1.9(1)
919.35(19)	0.23(4)
923.900(15)	25(1)
1047.731(25)	48(2)

---

[a] These γ-rays are subject to severe summing; consequently source-to-detector distances must be 10 cm or greater.

^{132}Cs (6.47d)

E_γ (ΔE_γ)	I_γ (ΔI_γ)
363.34(5)	0.71(4)
464.466(25)	16.0(2)
505.77(3)	5.5(2)
567.16(1)	2.2(1)
630.21(1)	8.2(4)
667.726(5)	1000(5)
687.74(17)	0.02(1)
772.61(1)	0.64(1)
1031.66(1)	1.43(4)
1135.010(25)	4.81(6)
1297.92(3)	0.69(2)
1317.928(12)	5.75(15)
1985.638(5)	0.82(12)

^{133}Ba (10.7y)

E_γ (ΔE_γ)	I_γ(ΔI_γ)
53.156(5)	34.8(7)
79.623(5)	37.7(9)
80.999(4)	512(4)
160.609(25)	10.5(3)
223.116(35)	7.1(2)
276.404(5)	113(2)
302.858(5)	292(3)
356.014(8)	1000(3)
383.859(6)	145(2)

^{34}Cs (2.062y)

$E_\gamma (\Delta E_\gamma)$	$I_\gamma (\Delta I_\gamma)$
242.90(5)	0.021(1)
326.46(10)	0.144(6)
475.36(5)	1.47(4)
563.27(5)	8.38(5)
569.30(3)	15.4(1)
604.68(2)	97.6(3)
795.78(2)	85.4(4)
801.86(3)	8.73(4)
847.0(2)	0.0003(1)
1038.53(5)	1.00(2)
1167.89(6)	1.81(3)
1365.17(10)	3.04(4)

^{149}Gd (9.4d)

$E_\gamma (\Delta E_\gamma)$	$I_\gamma (\Delta I_\gamma)$
40.877	1230(20)
41.529	2181(33)
47.027	705(47)
48.241	189(28)
125.98(1)	6.4(2)
128.75(3)	1.6(1)
132.001(9)	3.8(2)
138.09(2)	3.5(3)
149.736(3)	2043(14)
184.51(1)	1.90(7)
186.729(53)	0.42(5)
214.28	7.9(2)
252.222(4)	11.0(2)
260.737(6)	54.9(6)
264.63(3)	1.3(1)
272.317(5)	136(2)
278.28(2)	2.92(6)
298.634(5)	1178(5)
341.65(6)	3.2(3)
346.30(—)	3(1)
1000(3) {	
346.651(3)	997(3)
348.96(10)	4(1)
352.81(2)	1.8(3)
384.52(2)	3.2(1)
398.77(3)	1.8(1)
404.294(5)	8.5(2)
416.04(3)	0.92(8)
431.294(12)	2.9(2)
436.36(2)	2.7(1)
456.75(4)	0.9(1)
459.812(4)	24.5(2)
478.71(1)	9.7(2)
482.63(2)	3.2(2)
496.383(2)	70.1(3)
516.545(2)	113(2)
534.296(4)	131(1)
552.75(2)	3.5(2)
601.206	2.5(1)
645.315(2)	62.0(3)
662.89(1)	11.8(2)
666.290(4)	36.8(2)
726.16(4)	3.4(2)
734.84(2)	5.6(2)
748.601(2)	346(3)
788.878	309(3)
798.94(2)	1.9(1)
802.93(2)	1.8(1)
812.64(3)	6.2(1)
862.86(3)	2.87(9)
875.83(1)	6.4(1)
932.925(6)	26.3(2)
938.605(5)	101.5(1.2)
947.820(6)	40.3(7)
992.205(4)	1.35(4)
1012.59(5)	0.95(3)
1081.58(6)	0.74(3)
1096.70(5)	0.06(1)
1207.71(7)	0.045(4)
1231.0(2)	0.015(4)
1246.4(1)	0.091(7)

^{143}Ce (33.0h)

$E_\gamma (\Delta E_\gamma)$	$I_\gamma (\Delta I_\gamma)$
57.356(7)	270(10)
122.4(1)	0.8(1)
139.742(17)	1.8(1)
231.550(2)	48(1)
293.268(2)	1000(3)
328.777(58)	0.16(6)
350.619(3)	75.5(6)
371.292(29)	0.58(6)
389.636(18)	0.85(4)
416.57(10)	0.16(3)
432.999(6)	3.71(7)
438.434(76)	0.10(2)
446.021(85)	0.35(7)
447.452(18)	1.40(6)
490.368(5)	50.5(5)
497.809(21)	1.04(6)
556.873(13)	0.74(4)
569.909(85)	0.12(4)
587.196(15)	6.23(6)
614.216(30)	0.28(3)
664.571(15)	133(1)
670.121(58)	0.19(4)
675.5(5)	0.02(2)
682.817(85)	0.20(4)
709.590(49)	0.20(3)
721.929(13)	126(1)

^{143}Ce (33.0h) continued.

$E_\gamma (\Delta E_\gamma)$	$I_\gamma (\Delta I_\gamma)$
729.887(75)	0.05(1)
751.563(89)	0.057(6)
767.695(58)	0.074(8)
787.417(85)	0.05(1)
791.066(18)	0.31(1)
806.342(19)	0.67(2)
809.984(18)	0.73(2)
868.1(1)	0.08(2)
880.461(12)	24.1(2)
891.465(67)	0.19(2)
907.1(1)	0.03(1)
937.818(10)	0.61(3)
956.9(1)	0.03(1)
1002.852(12)	1.76(4)
1014.3(3)	0.03(1)
1031.217(25)	0.47(2)
1046.777(40)	0.28(2)
1060.217(16)	0.85(3)
1103.247(15)	9.7(1)
1160.582(57)	0.56(7)
1324.478(28)	0.037(1)
1340.091(89)	0.072(3)

^{150}Eu (35y)

$E_\gamma (\Delta E_\gamma)$	$I_\gamma (\Delta I_\gamma)$
370.721(25)	1.12(9)
372.728(25)	2.49(9)
377.728(27)	1.18(8)
381.990(26)	1.17(8)
402.152(12)	8.13(8)
403.36(10)	2.5(1)
406.518(50)	1.46(15)
420.55(22)	0.14(6)
439.401(15)	837(17)
448.789(12)	2.7(1)
453.578(99)	0.27(5)
458.363(61)	0.46(5)
461.761(15)	8.6(2)
464.114(72)	4.81(8)
474.498(25)	1.51(7)
476.89(13)	0.19(5)
485.931(20)	1.72(7)
505.521(25)	50(1)
509.843(48)	1.3(1)
515.792(5)	10.3(2)
520.085(19)	4.8(1)
540.545(59)	0.90(7)
542.972(25)	1.40(7)
553.198(97)	0.34(7)
571.259(15)	4.3(1)
575.514(75)	0.32(8)
584.274(12)	548(15)
590.71(11)	0.33(5)

^{150}Eu (35y) continued.

$E_\gamma (\Delta E_\gamma)$	$I_\gamma (\Delta I_\gamma)$
596.529(38)	0.77(7)
607.324(29)	1.74(5)
612.693(28)	0.97(6)
615.165(33)	0.84(4)
625.568(20)	3.23(7)
637.826(24)	0.15(7)
658.280(55)	0.55(5)
662.66(15)	0.16(4)
667.050(25)	2.7(1)
675.856(25)	5.3(1)
699.5(3)	0.06(4)
712.205(15)	11.3(3)
731.220(24)	3.5(1)
737.455(15)	100(2)
741.467(17)	8.9(1)
748.057(12)	54(1)
749.797(28)	7.0(1)
751.068(14)	22.3(5)
756.512(26)	1.18(7)
759.566(85)	0.80(7)
762.034(85)	0.29(5)
773.283(15)	6.3(1)
816.441(75)	0.51(5)
828.562(14)	6.1(2)
830.816(21)	5.54(12)
831.92(25)	0.7(2)
836.578(31)	3.2(1)
838.402(79)	0.6(1)
859.867(18)	6.1(1)
869.256(14)	19.3(2)
899.071(15)	9.8(1)
910.882(41)	0.9(1)
915.28(12)	0.17(7)
923.267(19)	3.2(1)
953.202(83)	0.47(7)
978.470(49)	0.21(5)
1045.873(12)	4.1(5)[a]
	6.3(5)
1049.043(25)	56(2)
1071.002(25)	1.5(1)
1081.460(78)	0.3(1)
1083.341(31)	1.7(1)
1115.35(26)	0.16(6)
1122.855(15)	3.5(1)
1165.739(27)	1.1(1)
1170.587(24)	13.9(2)
1193.826(24)	8.3(2)
1197.108(24)	11.8(4)
1246.968(24)	19.9(5)
1251.248(28)	1.7(1)
1261.978(27)	4.8(1)
1308.675(23)	9.3(2)
1321.912(27)	1.8(1)
1334.060(29)	4.3(1)
1343.777(22)	27.0(7)
1346.397(69)	0.30(7)

^{150}Eu (35y) continued.

$E_\gamma (\Delta E_\gamma)$	$I_\gamma (\Delta I_\gamma)$
1350.289(31)	1.8(1)
1379.118(55)	0.41(5)
1485.488(31)	19.8(8)
1499.35(10)	0.41(2)
1636.530(31)	7.5(1)
1690.668(17)	1.6(5)
1783.190(46)	1.07(3)
1818.517(75)	0.040(5)
1833.30(15)	0.027(5)

---

[a] Doublet.

^{152}Eu (13.4y)

$E_\gamma (\Delta E_\gamma)$	$I_\gamma (\Delta I_\gamma)$
121.783(2)	1362(16)
125.7(3)	0.57(9)
148.013(17)	1.9(4)
172.1(4)	0.02(1)
192.596(40)	0.33(1)
202.88(16)	0.18(9)
207.71(15)	0.21(6)
209.49(19)	0.21(6)
212.569(15)	0.94(3)
237.284(63)	0.45(4)
244.692(2)	359(6)
251.628(10)	3.0(1)
269.862(58)	0.39(4)
271.135(8)	3.5(1)
275.452(15)	1.61(5)
285.978(35)	0.53(5)
295.939(8)	21.1(5)
315.173(17)	2.43(6)
316.2(2)	0.10(6)
320.03(15)	0.08(3)
324.789(5)	3.6(1)
329.433(17)	5.9(1)
330.542(97)	3.6(5)
340.48(17)	1.3(3)
344.276(4)	1275(9)
351.666(36)	0.43(3)
357.259(50)	0.23(3)
367.789(5)	40.5(8)
379.36(18)	0.04(1)
385.52(17)	0.24(3)
387.903(81)	0.14(1)
391.32(14)	0.06(1)
406.74(15)	0.04(1)
411.115(5)	107(1)
416.052(6)	5.3(1)
423.449(89)	0.13(3)
440.856(95)	0.52(9)
443.976(5)	148(2)
482.303(29)	1.3(1)
488.661(39)	19.5(2)

^{152}Eu (13.4y) continued.

$E_\gamma (\Delta E_\gamma)$	$I_\gamma (\Delta I_\gamma)$
493.503(19)	1.9(1)
496.385(29)	0.44(3)
503.387(5)	7.3(1)
520.230(5)	2.57(7)
523.132(51)	0.071(4)
526.886(20)	0.63(3)
534.248(7)	2.06(5)
538.292(59)	0.20(3)
556.562(27)	0.91(5)
558.1(2)	0.19(4)
561.2(5)	0.05(1)
564.021(8)	23.6(5)
566.421(8)	6.2(1)
571.826(81)	0.23(4)
586.294(6)	22.0(5)
616.054(34)	0.43(4)
644.376(56)	0.28(4)
656.484(12)	6.9(1)
664.777(48)	0.9(1)
671.151(20)	1.1(1)
674.678(3)	8.9(3)
678.578(3)	22.1(4)
683.32(11)	0.15(4)
686.609(45)	0.92(8)
688.678(6)	40.0(8)
703.233(67)	0.25(4)
712.847(6)	4.6(1)
719.353(6)	15.6(3)
728.031(38)	0.54(5)
735.40(10)	0.28(5)
756.121(88)	0.26(4)
764.905(9)	8.4(4)
768.947(9)	4.3(4)
778.903(6)	619(8)
794.780(20)	1.18(6)
805.723(36)	0.61(5)
810.459(7)	15.2(2)
839.365(42)	0.79(5)
841.586(8)	7.8(1)
867.388(8)	199(4)
901.186(11)	4.4(3)
906.016(58)	0.72(6)
919.401(8)	20.9(5)
926.324(15)	12.7(4)
930.584(15)	3.5(1)
937.0(2)	0.15(5)
958.633(49)	1.1(1)
964.131(9)	692(9)
974.090(38)	0.69(5)
990.200(24)	1.48(6)
1001.1(3)	0.19(9)
1005.279(17)	31.0(7)
1084(1)	11.7(4)
1085.914(13)	475(7)
1089.700(15)	82(1)
1109.180(12)	8.8(2)

^{152}Eu (13.4y) continued.

$E_\gamma(\Delta E_\gamma)$	$I_\gamma(\Delta I_\gamma)$
1112.116(17)	649(9)
1139(1)	0.06(2)
1170.973(72)	1.71(6)
1206.09(16)	0.72(5)
1212.950(12)	67.0(8)
1249.946(13)	8.8(5)
1261.350(23)	1.57(6)
1292.784(19)	4.9(3)
1299.124(12)	78(1)
1348.09(7)	0.81(6)
1363.78(5)	1.17(5)
1390.4(2)	0.23(6)
1408.011(14)	1000(3)
1457.628(15)	23.6(5)
1528.115(19)	12.7(3)
1605.62(7)	0.36(3)
1608.355(79)	0.24(2)
1635.2(5)	0.007(2)
1674.310(57)	0.29(4)
1769.093(47)	0.42(3)

^{154}Eu$^+$ (8.2y)

$E_\gamma(\Delta E_\gamma)$	$I_\gamma(\Delta I_\gamma)^{a,b}$
123.14(4)	405(7)
188.22(4)	2.42(8)
248.04(4)	70.0(1.1)
401.30(5)	2.0(1)
444.40(5)	5.6(1)
478.26(5)	2.4(1)
557.56(5)	2.6(1)
582.00(5)	8.9(1)
591.75(4)	50.2(5)
625.23(5)	3.2(1)
676.60(5)	1.6(1)
692.42(4)	18.1(3)
715.77(5)	2.1(1)
723.31(4)	203(2)
756.88(5)	46.1(5)
815.57(5)	5.1(1)
845.41(5)	5.9(1)
850.66(5)	2.4(1)
873.21(5)	123(1)
892.75(5)	5.3(1)
904.07(5)	9.0(2)
996.35(4)	107(1)
1004.79(4)	184(2)
1118.53(6)	1.05(9)
1128.43(6)	3.14(9)
1140.93(7)	2.3(1)
1188.60(10)	0.9(1)
1241.62(9)	1.30(6)
1246.63(9)	8.8(1)
1274.42(7)	355(1)
1493.64(8)	7.06(10)

^{154}Eu$^+$ (8.2y) continued.

$E_\gamma(\Delta E_\gamma)$	$I_\gamma(\Delta E_\gamma)$
1537.84(5)	0.55(2)
1596.52(7)	18.2(3)

$^+$For a complete list of ^{154}Eu γ-rays, see R.A. Meyer, Phys. Rev. **170** (1968) 1089.

[a] Only γ-rays with an intensity of $I_\gamma > 10^{-3}$ per ^{154}Eu decay are listed. See above note.

[b] These intensities were obtained using the LLNL spectrometers and represent the average value. (See the discussion in Ref. 1).

^{155}Eu (4.9y)

$E_\gamma(\Delta E_\gamma)$	$I_\gamma(\Delta I_\gamma)$
18.784(35)	2.4(6)
26.532(21)	15.4(6)
31.4(1)	0.35(7)
45.295(13)	63(3)
57.986(30)	3.3(2)
60.022(15)	53.9(6)
86.554(15)	1496(30)
105.338(15)	1000(20)
146.090(90)	2.5(1)

^{182}Ta (115d)

$E_\gamma(\Delta E_\gamma)$	$I_\gamma(\Delta I_\gamma)$
31.737(1)	27.5(6)
42.716(2)	8.6(7)
65.722(1)	87.5(17)
67.750(1)	1310(100)^a
84.680(2)	71.9(14)
100.106(1)	404(5)
110.391(12)	3.0(2)
113.673(3)	53.4(5)
116.421(3)	12.6(2)
152.430(4)	199.5(1.8)
156.390(4)	75.9(1.0)
179.397(5)	88.2(1.0)
198.350(6)	41.9(9)
222.108(5)	216(3)
229.322(6)	103.9(1.8)
264.078(9)	102.6(1.8)
351.023(85)	0.34(8)
927.983(42)	17.3(3)
959.722(42)	9.8(3)
1001.696(18)	58.7(6)
1113.414(18)	13.2(3)

^{182}Ta (115d) continued.

$E_\gamma(\Delta E_\gamma)$	$I_\gamma(\Delta E_\gamma)$
1121.299(6)	1000(3)
1157.505(15)	29.2(3)
1189.051(6)	471(8)
1221.406(6)	778(13)
1223.2(1)	3(1)
1231.019(6)	331(5)
1257.421(6)	43.6(8)
1273.735(7)	19.5(3)
1289.158(6)	42.9(8)
1342.731(15)	7.4(1)
1373.838(10)	6.8(1)
1387.410(10)	2.7(1)
1411.077(45)	1.17(4)
1453.125(62)[b]	1.23(8)[b]

---

[a] X-rays interfere here.

[b] There are severe summing problems when the source-to-detector distance is less than 10 cm.

^{168}Tm (93.1d)

$E_\gamma(\Delta E_\gamma)$[a]	$I_\gamma(\Delta I_\gamma)$[b,c]
79.804(2)	201(1)[d]
87.73	0.03(2)
99.293(2)	(98.982) 2.8(4)[e] (99.289) 77.7(4)[e]
173.591(19)	0.77(5)
184.295(2)	333(3)
198.251(2)	1000(3)
221.8(5)	0.04(2)
272.896(13)	1.70(7)
284.655(14)	1.66(8)
348.509(2)	6.49(7)
422.305(7)	5.59(8)
447.510(2)	440(2)
497.782(58)	0.68(8)
511.00(15)	0.15(3)
521.134(66)	0.58(7)
546.805(30)	48.7(4)
557.083(12)	4.1(2)
559.5(4)	0.15(5)
568.8(4)	0.11(5)
582.57(25)	0.03(2)
620.59(7)	0.14(5)
631.705(3)	169.4(9)
645.766(3)	27.7(2)
673.670(15)	3.0(1)
720.379(4)	228(1)
730.660(4)	96.8(4)
737.7(7)	0.2(1)
741.355(4)	235(1)
748.282(7)	7.8(1)
(812.287)	(0.2)

^{168}Tm (93.1d) continued.

$E_\gamma(\Delta E_\gamma)$	$I_\gamma(\Delta I_\gamma)$
815.989(5)	935(3)
821.162(2)	220(1)
829.948(6)	128(1)
853.468(3)	0.63(3)
862.6(3)	0.027(15)
864	<0.001
914.933(4)	57.2(3)
928.916(7)	1.17(3)
1012.26(6)	0.21(2)
1014.226(10)	1.35(5)
1025.38)	0.0006(4)
1137.36(15)	0.008(4)
1167.357(6)	1.36(3)
1196.510(52)	0.074(9)
1229.08(11)	0.015(9)
1277.451(5)	30.9(2)
1279.100(23)	0.66(4)
(1310.03)	0.0012(9)
1323.909(9)	0.40(1)
1331.39(9)	0.015(4)
1351.575(5)	1.61(2)
1358.904(14)	0.19(1)
(1392.209)	<0.0004
1413.35(15)	0.008(2)
1431.68(38)	0.0068(15)
1461.750(4)	4.54(6)
1489.655(31)	0.039(2)
1493.7(2)	0.0037(6)
1541.56(3)	0.042(2)
1553.5(7)	0.0008(4)
1569.5(4)	0.0004(2)

---

[a] γ-ray emission probabilities given in parentheses are taken from n-capture γ-ray studies of W. F. Davidson and others (Ref. 25).

[b] These values are relative to the 198 keV γ-ray taken as 1000 units.

[c] Multiply by 0.0522 to convert to emission probability per 100 decays.

[d] In large volume Ge(Li) or high-purity Ge detectors this γ-ray may give an apparent intensity in the range of 190 to 208. This is due to several factors beyond the problem of correct efficiency description including summing and pulse pile-up loss.

[e] Intensity ratio of 1 to 28 for the intensity of the 98.982 to the 99.289 γ-ray determined using a LEPS detector and the computer code PEAKFIT by Gunnink and others (Refs. 9 and 10).

^{183}Re (70d)

$E_\gamma(\Delta E_\gamma)$	$I_\gamma(\Delta I_\gamma)$
40.977(1)	8(2)
46.485(1)	2520(140)
52.597(1)	699(35)
82.921(1)	80(2)
84.714(2)	275(16)
99.082(1)	850(35)
101.936(37)	4(1)
102.484(85)	0.8(4)
103.10(10)	1.3(6)
107.936(5)	687(30)
109.734(5)	915(30)
120.375(90)	1.0(2)
144.120(4)	37(1)
160.536(8)	186(7)
161.346(24)	114(15)
192.651(3)	81(2)
203.274(15)	14(1)
205.086(15)	35(1)
208.817(6)	939(20)
209.895(17)	70(1)
210.31(10)	3(2)
244.273(7)	130(3)
245.256(7)	81(12)
246.068(5)	417(12)
291.730(2)	1000(3)
313.029(5)	131(3)
354.077(15)	169(4)
365.623(9)	21(1)
406.603(16)	7.9(5)

^{185}Os (94d)

$E_\gamma(\Delta E_\gamma)$	$I_\gamma(\Delta I_\gamma)$
71.315(2)	31(8)
125.361(3)	43.1(4)
162.856(7)	69.3(7)
234.163(9)	51.4(7)
592.081(6)	164(1)
646.132(4)	10,000(30)
717.442(6)	509(2)
749.475(73)	0.40(5)
768.948(53)	0.45(4)
805.72(18)	0.005(4)
874.835(6)	816(4)
880.290(6)	617(3)
931.081(15)	6.1(2)

^{187}W (23.9h)

^{187}W (23.9h) continued.

$E_\gamma(\Delta E_\gamma)$	$I_\gamma(\Delta I_\gamma)$
16.61(2)	0.07(1)
29.23(3)	0.04(1)
40.92(5)	0.02(1)
43.66(6)	0.02(1)
72.46(1)	129(4)
77.37(5)	0.08(2)
93.22(5)	0.07(1)
100.14(2)	0.10(2)
106.59(1)	0.30(1)
113.75(2)	0.89(2)
123.79(11)	0.03(1)
134.22(1)	102(2)
138.50(6)	0.05(2)
165.67(40)	0.010(4)
168.50(40)	0.03(1)
198.34(12)	0.020(5)
206.29(3)	1.65(4)
208.29(3)	0.008(3)
239.04(3)	1.00(4)
246.19(1)	1.38(4)
275.62(12)	0.024(7)
352.87(17)	0.018(7)
374.32(14)	0.03(1)
375.94(13)	0.04(1)
454.93(2)	0.34(2)
479.54(1)	253(4)
484.15(3)	0.20(1)
492.8(2)	0.3(1)
511.76(1)	7.47(8)
551.55(1)	59(1)
564.63(19)	0.14(5)
573.72(14)	0.006(2)
576.32(8)	0.08(1)
578.73(11)	0.011(4)
589.11(3)	1.41(3)
612.9(4)	0.02(1)
618.39(1)	73(1)
625.54(1)	12.6(3)
638.67(2)	0.04(1)
647.3(3)	0.009(4)
682.3(2)	0.08(7)
685.83(1)	316(8)
693.1(2)	0.015(9)
745.23(2)	3.5(1)
767.4(8)	0.018(7)
772.89(2)	48(1)
816.58(2)	0.11(1)
825.0(3)	0.0027(4)
826.7(3)	0.0027(4)
844.7(5)	0.003(1)
864.57(1)	3.9(1)
879.45(5)	1.64(3)
960.19(5)	0.015(1)
1056.27(5)	0.0026(7)
1190.4(1)	0.0025(3)
1220.8(2)	0.0020(6)
1230.10(4)	0.0015(2)

References

1) R. A. Meyer, K. G. Tirsell and G. A. Armantrout, Lawrence Livermore National Laboratory Report UCRL-78222 (1976);
2) R. A. Meyer, *Multigamma-Ray Calibration Sources*, Lawrence Livermore National Laboratory Report M-100 (1978);
3) R. A. Meyer, *Gamma-Ray Calibration Sources*, Appendix to Table of Isotopes, C. M. Lederer & V. Shirley, Eds., J. Wiley Pub. Co., Inc., NY (1978);
4) J. Lin, E. Henry and R. A. Meyer, Lawrence Livermore National Laboratory Report UCRL-84536 (1980);
5) K. Debertin, Nucl. Instrum. and Meth. **158** (1979) 479;
6) Y. Yoshizawa, Y. Iwata, T. Kaku, T. Katoh, J. Ruan, R. Kojima and Y. Kawada, Nucl. Instrum. and Meth. **174** (1980A) 109;
7) Y. Yoshizawa, Y. Iwata and Y. Iiuma, Nucl. Instrum. and Meth. **174** (1980) 133;
8) R. Gunnink and J. B. Niday, Lawrence Livermore National Laboratory Report UCRL-51061, Vols. I—IV, (1971, 1972);
9) R. Gunnink and W. D. Ruhter, Lawrence Livermore National Laboratory Report UCRL-52917 (1980);
10) R. Gunnink, W. D. Ruhter and J. B. Niday, Lawrence Livermore National Laboratory, Nuclear Chemistry Div. Annual Report, FY 82, UCAR-10062-82/1 (1983);
11) R. Gunnink and J. B. Niday, Lawrence Livermore National Laboratory Report UCRL-76699 (1975);
12) R. Gunnink, *ERDA Symposium on Gamma-Ray Spectroscopy*, Univ. of Michigan (1976);
13) J. R. Van Hise, D. C. Camp and R. A. Meyer, Z. Physik **247** (1975) 322;
14) G. D. Loper and G. E. Thomas, Nucl. Instrum. and Meth. **105** (1972) 453;
15) F. M. Spits and J. Kopecky, Nucl. Phys. **A264** (1976) 63;
16) B. Krusche, K. P. Lieb, H. Daniel, T. von Egidy, G. Barreau, H. G. Borner and R. Brissot, Nucl. Phys. **A386** (1982) 245;
17) G. J. McCallum and G. E. Coote, Nucl. Instrum. and Meth. **124** (1975) 309;
18) E. G. Kessler, R. D. Deslattes, A. Henins and W. C. Saunders, Phys. Rev. Lett. **40** (1978) 171;
19) R. C. Greenwood, R. G. Helmer and R. J. Gehrke, Nucl. Instrum. and Meth. **77** (1970) 141;
20) R. G. Helmer, R. C. Greenwood and R. J. Gehrke, Nucl. Instrum. and Meth. **96** (1971) 173;
21) R. C. Greenwood, R. G. Helmer and R. J. Gehrke, Nucl. Instrum. and Meth. **159** (1979) 465;
22) W. M. Sanders and D. M. Holm, Los Alamos National Laboratory Report LA-4030 (1969);
23) P. Hoff, Phys. Scr. **21** (1980) 129;
24) J. Kern and W. Schwitz, Nucl. Instrum. and Meth. **151** (1978) 549;
25) W. F. Davidson, D. D. Warner, R. F. Casten, K. Schreckenbach, H. G. Borner, J. Simić, M. Stojanović, M. Bogdanovich, S. Koicki, W. Gelletly, G. B. Orr and M. L. Stelts, J. Phys. G. **7** (1981) 455; and Errata, J. Phys. G. **7** (1981) 843.

KALIBRACIONI STANDARDI VIŠESTRUKIH γ-ZRAKA

RICHARD A. MEYER

Division of Nuclear Physics, US Department of Energy, Washington, D. C. 20585, USA

i

Nuclear Chemistry Division, Lawrence Livermore National Laboratory, Livermore, California, USA

UDK 539.166

Originalni znanstveni rad

Kalibriran je konzistentni niz standarda višestrukih γ-zraka. Diskutirane su vjerojatnosti emisije γ-zraka za ^{149}Gd i ^{168}Tm izvore višestrukih γ-zraka.